Thermodynamic investigation of coordination-networked systems of [Mn_4] single-molecule magnets under pressure

2010 J. Phys.: Condens. Matter 22 026007

(http://iopscience.iop.org/0953-8984/22/2/026007)

J. Phys.: Condens. Matter **22** (2010) 026007 (6pp) doi:10.1088/0953-8984/22/2/026007

Thermodynamic investigation of coordination-networked systems of [Mn_4] single-molecule magnets under pressure

O Kubota[1], S Fukuoka[1], Y Nakazawa[1], K Nakata[2], M Yamashita[2] and H Miyasaka[2]

[1] Department of Chemistry, Graduate School of Science, Osaka University, Machikaneyama, Toyonaka, Osaka 560-0043, Japan
[2] Department of Chemistry, Graduate School of Science, Tohoku University, 6-3 Aramaki-Aza-Aoba, Aoba-ku, Sendai, Miyagi 980-8578, Japan

E-mail: nakazawa@chem.sci.osaka-u.ac.jp

Received 21 June 2009, in final form 29 October 2009
Published 14 December 2009
Online at stacks.iop.org/JPhysCM/22/026007

Abstract

Low temperature heat capacity measurements under pressure were performed for tiny single crystals of two-dimensional coordination-networked compounds consisting of [Mn_4] single-molecule magnets (SMMs) by the ac temperature modulation technique. Systematic variations of the peak temperature and the peak width of the thermal anomalies produced by pressure were clearly detected using two ruthenium oxide resistance chips in the Cu–Be clamp-type cell. A linear increase of the Néel temperature for an ordering set of large SMM spins with $S = 9$ was observed in $[Mn_4(hmp)_6\{N(CN)_2\}_2](ClO_4)_2$, while a non-monotonic variation of the peak temperatures and peak shapes was observed in $[Mn_4(hmp)_4Br_2(OMe)_2\{N(CN)_2\}_2](ClO_4)_2{\cdot}2THF{\cdot}0.5H_2O$ ($hmp^- =$ 2-hydroxymethylpyridinate; $N(CN)_2^- =$ dicyanamide as the linker among SMMs). We also report on thermodynamic behavior produced by changing external pressures and magnetic fields. The results are discussed in terms of the tilting angle of Ising axes in the two-dimensional plane.

(Some figures in this article are in colour only in the electronic version)

1. Introduction

Since the first observation of a ferromagnetic transition in the pure organic radical of the β-phase of p-NPNN (p-nitrophenyl-nitronyle-nitroxide) [1–3], numerous efforts have been made to realize characteristic properties based on molecular spins. To design new magnetic molecules with p- or d-electron spins and to arrange them in appropriate structures to have novel magnetic properties has been done by many synthetic chemists. The electron spins on these molecules can provide a rich variety of magnetic materials with different magnetic interactions from zero dimension (0D) to three dimension (3D). One of the successful examples in the past decade is the creation of single-molecule magnets (SMMs), which are magnetically isolated (0D) high-spin clusters containing multiple transition metal ions [4–6]. In SMM systems, high-spin clusters with uni-axial anisotropy has allowed them to exhibit nanometer-scale magnetic behavior. So naturally, a chemically linked compound of SMMs became the next target for a magnetic material that possibly has a character between an isolated SMM and a normal bulk magnet [7–9]. These compounds are constructed based on the idea of using SMM as a building unit for constructing a self-assembled network through coordination bonds. Using a double cuboidal [Mn_4] cluster possessing the SMM character as a building block and the dicyanamide anion as a linker, Miyasaka *et al* have succeeded in synthesizing 2D and 3D coordination-networked structures [7–9]. Since each [Mn_4] unit has a large spin with $S = 9$ in this cluster, a long-range magnetic order of giant magnetic moments to reach approx. 15 μ_B has been realized at relatively high temperatures of several kelvins even for weak exchange magnetic interactions J/k_B [9, 10].

Among several SMM-networked compounds which form quasi-2D structures, $[Mn_4(hmp)_6\{N(CN)_2\}_2](ClO_4)_2$ ($hmp^- =$ 2-hydroxymethylpyridinate) shows a long-range ordering at 4.35 K while $[Mn_4(hmp)_4Br_2(OMe)_2\{N(CN)_2\}_2](ClO_4)_2{\cdot}2THF{\cdot}0.5H_2O$ exhibits a rather broad transition around 2.03 K. The characterization of magnetic behaviors and the first heat capacity measurement of them is given in [9]. The detailed heat capacity measurements, including magnetic field dependences, are reported in the following papers [10, 11]. Although no ordering was observed for $[Mn_4(hmp)_4(pdm)_2\{N(CN)_2\}_2](ClO_4)_2{\cdot}1.75H_2O{\cdot}2MeCN$ (pdm^{2-} = pyridine-2,6-dimethanolate) in [9], the subsequent measurement by a dilution refrigerator detected an antiferromagnetic ordering around 0.38 K [11]. The series of heat capacity measurements have indicated that the magnetic orders have mainly arisen by the ground state doublet of $S_z = \pm 9$ through the evaluation of magnetic entropy around the transition temperatures. Since each constitutive unit is sensitive to magnetic fields owing to the large spin number and the strong Ising-type anisotropy, the long-range character is also suppressed when magnetic fields are applied parallel to the Ising axis direction. Rotation of the magnetic field in the plane at fixed temperatures also produces a change in thermodynamic behavior and therefore to control magnetic entropy by changing the magnitude and the direction of the magnetic field may be possible [10]. In addition, the application of a magnetic field also induces characteristic non-equilibrium behaviors with the long relaxation time and produces dynamic properties in magnetic behaviors, especially in the compounds with perpendicularly tilted Ising axes in the 2D plane. Actually, the glass-like transition in magnetic heat capacity in a weakly linked networked compound of $[Mn_4(hmp)_4(pdm)_2\{N(CN)_2\}_2](ClO_4)_2{\cdot}1.75H_2O{\cdot}2MeCN$ is reported as a sudden drop of heat capacity at 0.9 K [11].

In these networked compounds, the SMM units have magnetic interactions through coordination ligands of dicyanamide. Because of the flexibility of the ligands, the compounds have relatively soft lattices as compared with many intermetallic compounds like transition metal oxides. Interestingly, variations of magnetic characters by application of pressure has been reported in [12] by ac susceptibility measurements under pressure.

With a backing of these magnetic characteristics, it is the aim of this work to pursue the entropic change of the magnetic characteristics due to external pressure using a single-crystal sample. Although numerous experiments such as magnetic, transport, optical and structural have been performed for molecular magnets under pressure, thermodynamic measurements have not yet been performed. We have recently reported a technique to measure heat capacities of single-crystal samples [13]. In our preliminary experiment in [13], we have confirmed that the measurement of the $[Mn_4]$ cluster compound is possible by this method. Throughout the systematic thermodynamic measurements under hydrostatic pressures and with external magnetic fields of the $[Mn_4]$ networked system, an interesting shift of the peak temperature and peak width in heat capacity has been observed and discussed from the entropic standpoint for the first time.

2. Experimental details

The target materials for the high pressure experiments in this study are $[Mn_4(hmp)_6\{N(CN)_2\}_2](ClO_4)_2$ and $[Mn_4(hmp)_4Br_2(OMe)_2\{N(CN)_2\}_2](ClO_4)_2{\cdot}2THF{\cdot}0.5H_2O$ which are coordination network compounds of $[Mn_4]$ clusters. The $[Mn_4]$ clusters are arranged in 2D networked structures, as shown in figure 1. The samples were synthesized by Tohoku University according to the procedure described in [9]. We used a single crystal weighing 239.4 μg for $[Mn_4(hmp)_6\{N(CN)_2\}_2](ClO_4)_2$ and one weighing 105.9 μg for $[Mn_4(hmp)_4Br_2(OMe)_2\{N(CN)_2\}_2](ClO_4)_2{\cdot}2THF{\cdot}0.5H_2O$. The former shows a distinct long-range antiferromagnetic transition at 4.35 K, while the latter shows a broad peak at 2.03 K from the single-crystal relaxation calorimeter. In the schematic structure shown in figure 1, we compare the difference in tilting angle θ between the two kinds of Ising axes in the network plane of both compounds. The tilting angle θ is 18° for $[Mn_4(hmp)_6\{N(CN)_2\}_2](ClO_4)_2$ and 63° for $[Mn_4(hmp)_4Br_2(OMe)_2\{N(CN)_2\}_2](ClO_4)_2{\cdot}2THF{\cdot}0.5H_2O$. The details of the crystal structure and magnetic properties of these materials are reported in [9].

The heat capacity measurement under pressure was performed by the low temperature ac technique [13]. The basic concept of this method was proposed by Eichler and Gey in 1979 [14]. Although their apparatus was designed for measuring samples of the order of 10^2 mg, we have modified it for detecting the signal of tiny crystals of organic compounds. We used two different chip-type resistances of ruthenium oxides (KOA Co. Ltd) whose room temperature resistance was 100 Ω, 1 kΩ. The former was used for a sensor and the latter was used for a thermometer. Single crystals $1.6 \times 0.7 \times 0.2$ mm^3 for $[Mn_4(hmp)_6\{N(CN)_2\}_2](ClO_4)_2$ and $1.5 \times 0.6 \times 0.15$ mm^3 for $[Mn_4(hmp)_4Br_2(OMe)_2\{N(CN)_2\}_2](ClO_4)_2{\cdot}2THF{\cdot}0.5H_2O$ are sandwiched between these chips. The sample with the heater and the thermometer is coated by epoxy to ensure temperature stability around the sample. Hydrostatic pressures up to 1.1 GPa were applied using a CuBe clamp-type cell with a Daphne 7373 pressure medium. The ac current supplied to the heater resistance produces temperature modulation around the sample which can be detected as a modulation of the sensor resistance. This modulation was recorded as an error signal from setpoint values of the ac resistance bridge. The suitable frequency region for performing ac calorimetry was investigated in detail in [13] and 25–40 Hz was concluded to be appropriate for these samples. The validity of the measurements was confirmed by measuring the pressure dependence of the superconductive transition of indium metal with a diameter of ⌀1 mm and thickness of 0.5 mm. The detected ac modulation signals were transformed into the heat capacity after correcting for the temperature dependence of the heater and thermometer chip resistances. The calorimetry cell was mounted on a ^{3}He refrigerator which can be inserted in an 8 T superconducting magnet. By this technique, it is possible to derive thermodynamic information by controlling external pressures and magnetic fields.

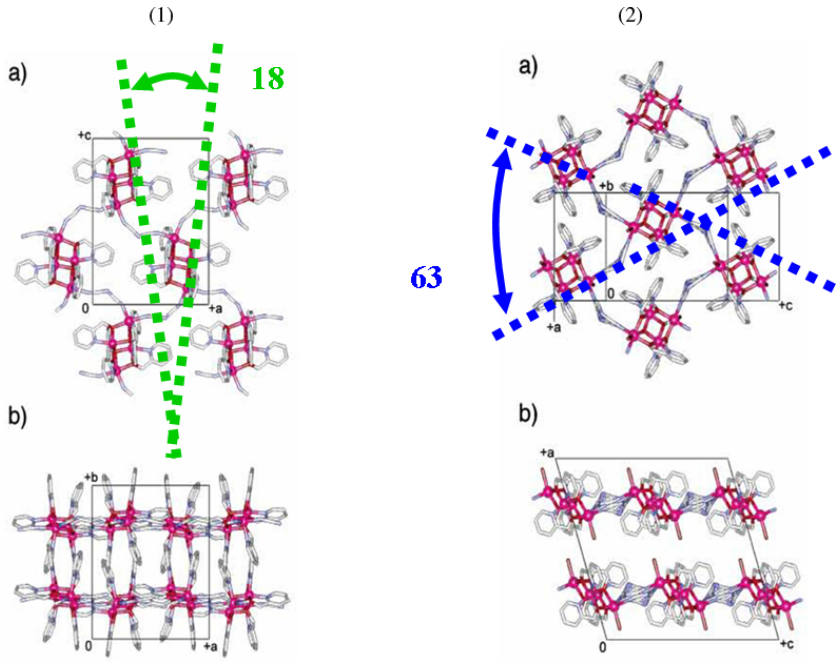

Figure 1. Crystalline structure of (1) $[Mn_4(hmp)_6\{N(CN)_2\}_2](ClO_4)_2$ and (2) $[Mn_4(hmp)_4Br_2(OMe)_2\{N(CN)_2\}_2](ClO_4)_2{\cdot}2THF{\cdot}0.5H_2O$. The arrangement of $[Mn_4]$ cluster units in the 2D plane is shown in (a) and the inter-planar structure is shown in (b) for both compounds. The directions of the two kinds of Ising-type axes of SMM units in the sheet are shown by the broken lines.

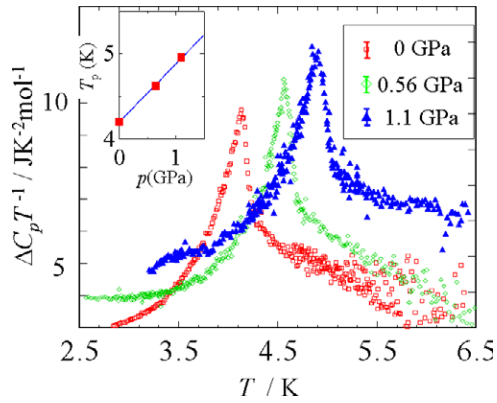

Figure 2. Temperature dependence of heat capacity of $[Mn_4(hmp)_6\{N(CN)_2\}_2](ClO_4)_2$ obtained under various pressures. The inset graph shows the shift of the peak temperature by external pressure. The magnitude of the error bars is shown with explanatory remarks in the other inset.

3. Results and discussion

3.1. $[Mn_4(hmp)_6\{N(CN)_2\}_2](ClO_4)_2$ *system*

In figure 2, we show temperature dependences of the heat capacity of $[Mn_4(hmp)_6\{N(CN)_2\}_2](ClO_4)_2$ obtained under pressures of 0, 0.56 and 1.1 GPa. The sharp distinct peak at which magnetic entropy has been estimated to be $1.1R\ln 2$ at 5 K, as is reported in [10], shifts to the higher temperature side with the increase of pressure. The peak is not broadened and keeps the same width even under a high pressure of 1.1 GPa. These results reveal that the homogeneity of the pressure is attained in the measurement. Although it is very difficult to achieve absolute precision of the measurement owing to the large additional contribution by the thermometer and heater chip and the heat release through the pressure medium, the resolution attained in this method is appropriate to grasp the systematic change of the magnetic order. From the previous relaxation calorimetry using the same materials, the application of 2 T reduces the long-range order due to the large Zeeman effect of $S = 9$ spins [10]. Therefore, by subtracting the data of 2 T from those of 0 T, we can calibrate the heat capacity signal using the absolute value of the relaxation calorimetry results. The values of the vertical axis in figure 2 were thus determined in order to evaluate the peak height and the magnetic entropy. As is shown in the inset, the Néel temperature determined by the heat capacity peak increases linearly against the external pressure with a slope of $dT_N/dp = 0.068$ kGPa^{-1}. In spite of this linear increase, the peak shape scales well if we plot the data in C_pT^{-1} versus T/T_{peak}, as is shown in figure 3. This result means that the magnetic entropy related to the transition is not affected by the systematic change of magnetic interaction induced by pressures. The shift of the peak temperature demonstrates that the magnetic interaction increases with the decrease of the intercluster distance, which is a typical behavior of magnetic materials with long-range ordering. Since the magnetic order has an Ising-type nature of 2D in this compound, the nearest-neighbor interactions by way of dicyanamide linkers may dominate the magnetic order, although the possibility of the dipole interaction cannot be excluded as a possible origin of the ordering. The effective magnetic coupling between $[Mn_4]$ spins is estimated from the critical magnetic field, $Hc(0)$, through the formula in equation (1) in [9]. Taking account of this formula, the effective magnetic interaction between

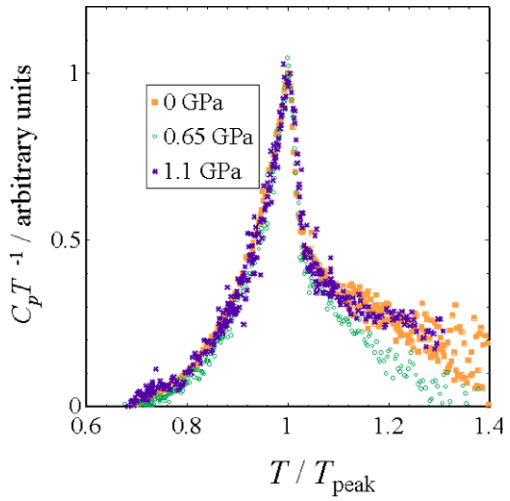

Figure 3. The scaling relation of the heat capacity peak against T/T_{peak}.

$[Mn_4]$ clusters can be discussed in relation to the tilting angle between two Ising axes in the 2D sheet. The interaction gives a maximum value in the parallel configuration. Probably, the increase of pressure works to make the tilting axis smaller and therefore the effective exchange coupling between neighboring spins increases with the increase in pressure.

Experiments performed by Wada *et al* [15] using the adiabatic technique under various pressures for $CoCl_2{\cdot}6H_2O$ with antiferromagnetic ordering shows a linear increase of the peak temperatures. A similar behavior is observed in the organic radical ferromagnet of 2,5-DEPNN [16, 17]. Although these studies were performed for polycrystal or powder samples, the qualitative resemblance of the peak shift in the present system ensures that the pressure works to increase the magnetic interaction J/k_B of neighboring spins. The pressure dependence of the heat capacity observed here means that the external pressure drastically affects the linkage of the dicyanamide ligands.

3.2. The $[Mn_4(hmp)_4Br_2(OMe)_2\{N(CN)_2\}_2](ClO_4)_2{\cdot}2THF{\cdot}0.5H_2O$ *system*

The pressure dependence of the thermodynamic peak of $[Mn_4(hmp)_4Br_2(OMe)_2\{N(CN)_2\}_2](ClO_4)_2{\cdot}2THF{\cdot}0.5H_2O$ is different from that of $[Mn_4(hmp)_6\{N(CN)_2\}_2](ClO_4)_2$. At ambient pressure, the broad heat capacity peak around 2.03 K reported in [9, 10] is reproduced well in this measurement by the high pressure calorimeter. With the increase of pressure, we have observed that the peak shape and the peak temperature change moderately but non-monotonically, as is shown in figure 4. In order to discuss the peak shape quantitatively, we performed a similar calibration as for $[Mn_4(hmp)_6\{N(CN)_2\}_2](ClO_4)_2$ using the difference between 0 and 2 T data. The vertical axis corresponds to the magnetic contribution defined as $\Delta C_pT^{-1} = (C_p(0\ \mathrm{T}) - C_p(2\ \mathrm{T}))/T$. The data under pressure plotted in figure 4(a) is shifted by a constant value of 1.5 J K^{-2} mol^{-1} with the increase of pressure to avoid the overlap of the data points in the same figure.

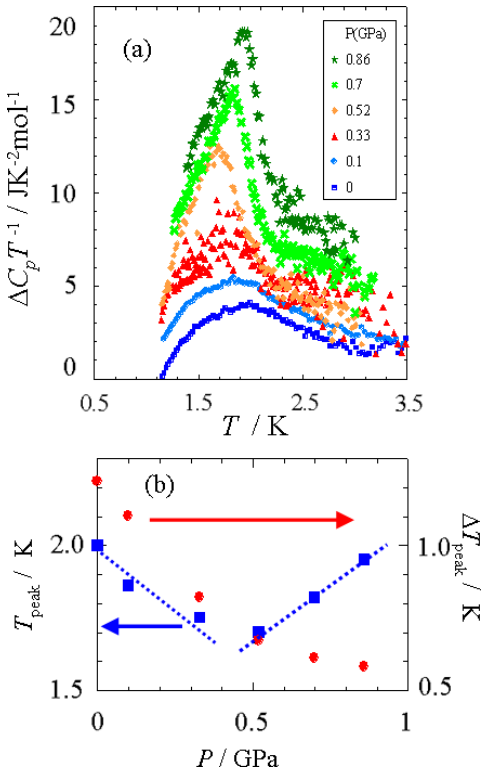

Figure 4. (a) Temperature dependence of magnetic heat capacity of $[Mn_4(hmp)_4Br_2(OMe)_2\{N(CN)_2\}_2](ClO_4)_2{\cdot}2THF{\cdot}0.5H_2O$. (b) The shift of the peak temperature and the peak width of $[Mn_4(hmp)_4Br_2(OMe)_2\{N(CN)_2\}_2](ClO_4)_2{\cdot}2THF{\cdot}0.5H_2O$ under pressure.

The systematic change of the peak temperature and the peak shape is observed clearly in figure 4(a). With the increase in pressure, the peak temperature decreases gradually and the broad peak at ambient pressure is further broadened up to about 0.52 GPa. The shift of the peak temperature is shown in figure 4(b), which gives a minimum value of 1.7 K at 0.52 GPa. Interestingly, by further increasing the pressure above 0.52 GPa, the peak temperature increases and reaches 1.95 K at 0.86 GPa. We also show the variation of the half-width of the peak in figure 4(b), where we can find that the peak is broadened once but recovers to be sharp again with the increase in pressure. The sharper peak in the high pressure region means that the long-range nature is enhanced, as in the case of $[Mn_4(hmp)_6\{N(CN)_2\}_2](ClO_4)_2$. The slope of dT_N/dp above 0.52 GPa is 0.072 $kGPa^{-1}$, which is close to the slope of $[Mn_4(hmp)_6\{N(CN)_2\}_2](ClO_4)_2$. The suppression of the ordering temperature and its subsequent recovery is reported by Ogawa *et al* through the ac susceptibility under pressure [12]. They suggested that the broad transition is suppressed once and the SMM-like character becomes dominant in the low pressure region. They also observed that the bulk magnet behavior recovers in the higher pressure region. These results are quite consistent with the present thermodynamic behavior observed in this work. We cannot explain the reason for the data scattering at 0.33 GPa, but we have observed the same tendency in the different samples performed independently. Since our method is an ac

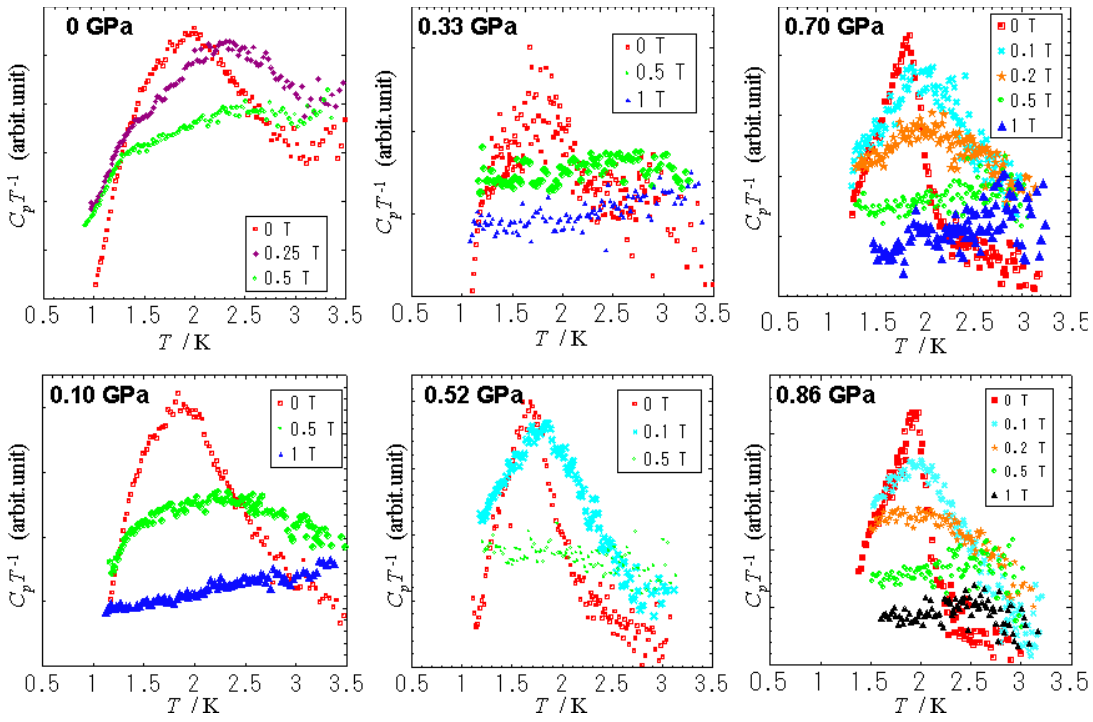

Figure 5. Magnetic field dependence of the heat capacity peak structures of $[Mn_4(hmp)_4Br_2(OMe)_2]\{N(CN)_2\}_2\cdot 2THF\cdot 0.5H_2O$ measured under ambient pressure, 0.10, 0.33, 0.52, 0.70 and 0.86 GPa.

calorimetry with a modulation frequency of 25–40 Hz, spin dynamics related to the SMM character grows in this frequency region. To study the systematic frequency dependence down to the dc region is necessary for further understanding, since the SMM behaviors should be detectable by ac calorimetry in the lower frequency region. An important fact to be emphasized here is that the magnetic entropy appears to remain at $R\ln 2$ corresponding to the full entropy of the magnetic ground state of $S_z = \pm 9$, although the peak shape changes drastically under pressure.

The origin of the minimum of the peak temperature and the non-monotonic behavior across 0.52 GPa may be attributable to the change in tilting angle, as we have discussed above. The external pressure works to change the tilting angle, and therefore affects the nearest-neighbor magnetic interactions J/k_B between $[Mn_4]$ spins. In the weak pressure region, the tilting angle of 63° increases to weaken the magnetic interactions. However, when the pressure is larger than 0.52 GPa, two Ising axes tend to be parallel, as in the case of $[Mn_4(hmp)_6\{N(CN)_2\}_2](ClO_4)_2$. In order to confirm this tendency, we show the heat capacity results performed in a combination of magnetic fields and external pressures. The magnetic field dependences of heat capacities at 0, 0.10, 0.33, 0.52, 0.70 and 0.86 GPa are shown in figure 5. In these measurements, the magnetic fields are applied almost parallel to the *b*-axis in the 2D network. In the high pressure regime of 0.70 and 0.86 GPa, where the peak shape is sharp, the magnetic field of approximately 0.5 T suppresses the order completely. On the other hand, in the ambient pressure data shown in [10] and those in 0.10 GPa, the peak is broadened but remains at 0.5 T. The behavior of the heat capacity peak against magnetic fields of 0.70 and 0.86 GPa resembles the case of $[Mn_4(hmp)_6\{N(CN)_2\}_2](ClO_4)_2$, where the Ising axis is almost aligned in one direction and the heat capacity peak disappears when external fields are applied parallel to the Ising axis.

In ambient pressure, two Ising axes of $[Mn_4(hmp)_4Br_2(OMe)_2\{N(CN)_2\}_2](ClO_4)_2\cdot 2THF\cdot 0.5H_2O$ have a large tilting angle and therefore the application of magnetic fields does not give anisotropic behavior when the magnetic fields are applied in different directions in the 2D plane. However, when the external pressures above 0.25 GPa are applied, Ogawa and Mito *et al* suggested that the contraction of the *c*-axis is larger when compared with that of the *b*-axis [12]. According to the preliminary work by them, the contraction of the *c*-axis is almost negligible up to 0.75 GPa, while nearly 2.5% contraction in the *b*-axis is observed at this pressure by x-ray analysis. The data will be published by their group elsewhere. Taking account of this behavior, it is suggested that the crystal structure changes such that the tilting angle becomes smaller and the two Ising-type axes tend to be aligned in the *b*-axis direction. The increase of the transition temperature and an appearance of the shaper peak revealed in this region are consistent with this tendency. Although this is still a speculative discussion, the result means that the direction of Ising axes in the high pressure regime are inclined to be close to the behavior of $[Mn_4(hmp)_6\{N(CN)_2\}_2](ClO_4)_2$, which has the character of a bulk magnet. It is important to perform similar experiments by applying magnetic fields in the *c*-axis direction as well as in the *b* direction. However, to obtain data for different pressures and magnetic fields is not so easy owing to many experimental restrictions which should be performed inside the pressure cell. The experiment by adjusting the *c*-axis direction in our calorimetric set-up is not successful at present

due to the lack of space inside the pressure cell. We consider that to report the systematic change of the peak temperature and peak width is necessary in the future.

In the lower pressure region where the tilting angle is close to the perpendicular arrangement, the antiferromagnetic ordered structure of large magnetic moments is not so stable and a kind of frustration is produced in the plane. This instability produces short-range fluctuations which lead to a dynamic character like SMM systems. The tuning of magnetic character using external parameters can give the possibility of deriving interesting phenomena in these SMM-networked compounds.

4. Conclusion

We have performed thermodynamic investigations for $[Mn_4]$ networked compounds under pressure and with magnetic fields using small single crystals. The systematic increase of long-range order with the increase of pressure was clearly detected by heat capacity in $[Mn_4(hmp)_6\{N(CN)_2\}_2](ClO_4)_2$. However, non-monotonic changes in the peak temperature and peak shape appear in $[Mn_4(hmp)_4Br_2(OMe)_2\{N(CN)_2\}_2](ClO_4)_2{\cdot}2THF{\cdot}0.5H_2O$. The results are discussed in relation to the tilting angles of Ising axes in the 2D plane. These results imply the importance of the high pressure calorimetry of the molecular magnet using single crystals and that the application of the method to various materials is promising in condensed matter science, especially for the field of molecular magnetism. The combination of two external parameters to control the magnetic peak gives us the possibility to extend the thermodynamic discussion to a universal level. To derive a universal relation including the pressure and magnetic fields in different directions will be a future goal for thermodynamic work on these series of materials.

Acknowledgments

This study was supported by the CREST project 'Creation of Quantum Nano-Magnets' through the Japan Science and Technology Agency (JST) and partially supported by a Grant-in-Aid on Priority Area 'Novel States of Matter Induced by Frustration' from the Ministry of Education, Science, Sports and Culture of Japan. One of the authors (YN) would like to thank the Casio Foundation for providing financial support.

References

[1] Tamura M, Nakazawa Y, Shiomi D, Nozawa K, Hosokoshi Y, Ishikawa M, Takahashi M and Kinoshita M 1991 *Chem. Phys. Lett.* **186** 401
[2] Kinoshita M, Turek P, Tamura M, Nozawa K, Shiomi D, Nakazawa Y, Ishikawa M, Takahashi M, Awaga K, Inabe T and Maruyama Y 1991 *Chem. Lett.* **20** 1225
[3] Nakazawa Y, Tamura M, Shirakawa N, Shiomi D, Takahashi M, Kinoshita M and Ishikawa M 1992 *Phys. Rev.* B **46** 8906
[4] Christou G, Gatteschi D, Hendrikson D N and Sessoli R 2000 *MRS Bull.* **25** 66
[5] Gatteschi D and Sessoli R 2003 *Angew. Chem. Int. Edn* **42** 268
[6] Coronado E, Palacio F and Veciana J 2003 *Angew. Chem. Int. Edn* **42** 2570
[7] Miyasaka H, Nakata K, Sugiura K, Yamashita M and Clérac R 2004 *Angew. Chem. Int. Edn* **43** 707
[8] Miyasaka H and Yamashita M 2007 *Dalton Trans.* **399**
[9] Miyasaka H, Nakata K, Lecren L, Coulon C, Nakazawa Y, Fujisaki T, Sugiura K, Yamashita M and Clérac R 2006 *J. Am. Chem. Soc.* **128** 3770
[10] Fujisaki T, Nakazawa Y, Oguni M, Nakata K, Yamashita M, Lecren L and Miyasaka H 2007 *J. Phys. Soc. Japan* **76** 104602
[11] Yamashita S, Fujisaki T, Nakazawa Y, Oguni M, Nakata K, Yamashita M and Miyasaka H 2008 *J. Phys. Soc. Japan* **77** 073708
[12] Ogawa M, Mito M, Tajiri T, Deguchi H, Takagi S, Nakata K, Yamashita M and Miyasaka H 2007 *J. Magn. Magn. Mater.* **310** e489
[13] Kubota O and Nakazawa Y 2008 *Rev. Sci. Instrum.* **79** 053901
[14] Eichler A and Gey W 1979 *Rev. Sci. Instrum.* **50** 1445
[15] Wada M, Takeda K, Ohtani A, Onodera A and Haseda T 1983 *J. Phys. Soc. Japan* **52** 3188
[16] Mito M, Deguchi H, Tanimoto T, Kawae T, Nakatsuji S, Morimoto H, Anzai H, Nakano H, Murakami Y and Takeda K 2003 *Phys. Rev.* B **67** 024427
[17] Ito M, Yamashita H, Kawae T and Takeda K 1997 *J. Phys. Soc. Japan* **66** 1265